



IMF²O²: A Fully Connected Sensor Deployment Algorithm for Underwater Sensor Networks

NA XIA, YIN WANG, BIN CHEN, and HUAZHENG DU, Hefei University of Technology, China
CHAONONG XU, China University of Petroleum, China
RONG ZHENG, Mc Master University, Canada

To address the problems of node deployment schemes in existing underwater sensor networks that lack consideration of network connectivity and high deployment costs, this article constructs an optimization model that maximizes network coverage and minimizes deployment costs while ensuring full connectivity. For the NP-hard property of this optimization model, an improved moth flame optimization node deployment algorithm based on fuzzy operators (IMF²O²) is proposed. First, comprehensively considering the two performance metrics of network coverage and network connectivity, a multi-objective selection mechanism based on fuzzy operators is proposed to improve network coverage while ensuring full connectivity. Second, a fixed number of nodes are used to monitor the target event points, transforming the node deployment of sensors into an optimal problem and proposing an improved moth flame optimization algorithm to solve this problem. Finally, the two metrics of coverage and deployment cost are measured and the fuzzy operator is used to select the optimal number of nodes to be deployed. Numerical results showed that the proposed algorithm improved network coverage rate by 10%, 22%, and 25%, and improved network connectivity rate by 12%, 20%, and 8% as compared to PSSD, RAWs, and VODA, respectively, while ensuring full connectivity.

CCS Concepts: • **Networks** → **Network architectures**; *Network algorithms*;

Additional Key Words and Phrases: Underwater Sensor Networks (UWSNs), deployment, fuzzy operator, improved moth flame algorithm, fully connected

ACM Reference format:

Na Xia, Yin Wang, Bin Chen, Huazheng Du, Chaonong Xu, and Rong Zheng. 2023. IMF²O²: A Fully Connected Sensor Deployment Algorithm for Underwater Sensor Networks. *ACM Trans. Sensor Netw.* 19, 3, Article 67 (March 2023), 22 pages.

<https://doi.org/10.1145/3577201>

This work was support in part by the National Natural Science Foundation of China under Grant 61971178 and Grant 61701161; in part by Science and Technology Major Project of Anhui Province under Grant 18030901015; in part by Demonstration of Comprehensive Application of Beidou in Anhui Province under Grant ZF2022-08-0020, and Special Project A for Young Faculty Research Innovation under Grant JZ2020HGQA0185.

Authors' addresses: N. Xia, Hefei University of Technology, No. 485 Danxia Road, Hefei, China, 230009; email: xiananawo@hfut.edu.cn; Y. Wang (corresponding author), B. Chen, and H. Du, Hefei University of Technology, No. 485 Danxia Road, Hefei, Anhui, China, 230009; emails: wangyin950203@gmail.com, {bin.chen, dhz2016}@hfut.edu.cn; C. Xu, China University of Petroleum, No. 18 Fuxue Road, Beijing, China, 102249; email: xuchaonong@cup.edu.cn; R. Zheng, Mc Master University, 1280 Main Street West, Hamilton, Canada, L8S4K1; email: rzheng@uh.edu.

Permission to make digital or hard copies of all or part of this work for personal or classroom use is granted without fee provided that copies are not made or distributed for profit or commercial advantage and that copies bear this notice and the full citation on the first page. Copyrights for components of this work owned by others than ACM must be honored. Abstracting with credit is permitted. To copy otherwise, or republish, to post on servers or to redistribute to lists, requires prior specific permission and/or a fee. Request permissions from permissions@acm.org.

© 2023 Association for Computing Machinery.

1550-4859/2023/03-ART67 \$15.00

<https://doi.org/10.1145/3577201>

1 INTRODUCTION

Underwater sensor networks (UWSNs) are widely used in marine data collection, environmental pollution monitoring, marine sampling, assisted navigation, tsunami and earthquake early warning systems, and other domains, which have gained the attention of the scientific and industrial communities [6, 19, 34]. In recent years, with the rapid development of **wireless sensor networks (WSNs)** technology, research on UWSNs has mainly involved underwater acoustic or optical communication technology [9, 11, 45], node deployment and networking [13, 25, 33, 36], data collection [39, 43, 47], routing protocol [4, 14, 27, 42, 44], and location tracking [5, 12]. The deployment of underwater sensor nodes can affect node positioning and lifetime, which are key factors affecting the performance of UWSNs. Therefore, studying the deployment of underwater sensor nodes has important significance.

Although there are many effective technologies for conventional WSNs, UWSNs use acoustic or optical communication and have limited communication bandwidth, high bit error rate, and high latency compared to conventional WSNs. Therefore, it is essential to develop new solutions for node deployment. In terms of deployment methods, existing UWSN deployment schemes are broadly classified into static, restricted mobility, and free mobility deployment. Static deployment means that the sensor is fixed to a known position, which has the advantages of simplicity and convenience, but the position cannot be changed. Restricted mobility deployments allow vertical depth adjustment, reducing redundancy between nodes and improving coverage efficiency. In a free mobile deployment, nodes can move in all directions as required to maximize coverage, but this is more costly and technically challenging.

Network coverage and network connectivity are two of the most important performance metrics for node deployment. The optimization goal of existing research schemes only has considered maximizing coverage, ignoring the connectivity between nodes, or increasing deployment density to achieve full connectivity, ignoring hardware costs. Based on this research status, this article proposes a deployment method for target monitoring points in a 3D underwater environment. Specifically, this work contains the following contributions:

- We propose an optimization model that maximizes network coverage and minimizes deployment costs while ensuring full connectivity.
- Addressing the NP-hard property of the optimization model, an improved moth flame optimization node deployment algorithm based on fuzzy operators (IMF²O²) is proposed. A multi-objective selection mechanism based on fuzzy operators is designed to maximize coverage with a guaranteed connectivity of 1. The optimal number of nodes to be deployed is selected by the fuzzy operator, measuring the two metrics of coverage and deployment cost.
- We propose an **improved moth flame algorithm (IMFO)** to improve the target coverage and network connectivity rate of node deployments, addressing the problem that traditional moth flame algorithms tend to fall into local optimum solutions.

The rest of the article is organized as follows: Section 2 provides background information and related work. Section 3 describes the UWSNs-related model and problem definition related to UWSNs. Section 4 proposes a fuzzy operator-based multi-objective selection mechanism and IMF²O². Section 5 presents the detailed experimental results and analyses. We conclude the article in Section 6.

2 RELATED WORK

In this section, we analyze the related work on node deployment for WSNs and UWSNs. According to the different scopes of node deployment, the research and development of UWSNs

node deployment methods are divided into two categories: deployment methods for specific underwater sensor nodes and methods for all underwater sensor nodes.

2.1 Deployment of Wireless Sensor Networks

To dynamically deploy the sensor node of the WSN in 3D terrain, Du et al. [8] proposed a new method based on a combination of the distributed particle swarm optimization algorithm and a proposed 3D virtual force algorithm. The proposed sensor deployment algorithm can improve the coverage and guarantee the connectivity of a WSN. However, the cost of deploying the optimum number of nodes was not considered. Gupta et al. [10] proposed an optimal deployment model in terms of the number of nodes required to achieve k -coverage in an m -connected WSN. Divide the irregular interest domain into regular patterns, such as triangles, squares, and hexagons, and estimate the optimal distance between nodes and patterns to achieve k -coverage in m -connected WSN. However, this deployment scheme is based on 2D area division and is not suitable for underwater node deployment scenarios. To address the problems of poor network connectivity and sensing coverage in the deployment of stochastic WSNs, Olasupo et al. [32] proposed the hierarchical logical mapping and deployment method. The algorithm uses a disk communication model and radio frequency propagation model to optimize sensing and connectivity coverage. To further complete the optimization method, the study utilizes efficient image processing algorithms to classify the deployment terrain to improve deployment and connection coverage at the required minimum number of nodes and transmission parameters. However, the deployment scheme of this method is based on 2D area division and is not applicable to underwater acoustic channels.

Hao et al. [15] proposed a 3D coverage deployment method based on received signal strength in a probabilistic model. First, the threshold of path loss is set to define the maximum distance between nodes, which further ensures the connectivity and prolongs the lifecycle of the network. Then, an improved particle swarm optimization algorithm is used to solve the optimal coverage deployment problem. On the premise of ensuring network connectivity, an adaptation function suitable for 3D WSNs is adopted, and the local optimum can be jumped out according to the cooling operation of a simulated annealing algorithm. However, the algorithm maximizes the 3D spatial node coverage with guaranteed connectivity in advance but does not consider the cost of deploying the necessary number of nodes. To achieve an optimal balance between WSN lifetime, cost, coverage, connectivity, and fault tolerance, Ng et al. [31] proposed a two-phase deployment strategy. In the first stage, the sensor node deployment is determined by a mathematical model that optimizes two objectives: area coverage quality and cost of deployment. The second-stage relay node deployment model is set to optimize three objectives: connection quality, fault tolerance quality, and number of deployed relay nodes. To implement the strategy, they proposed a bat algorithm-based meta-heuristic algorithm named smart bat algorithm. The method for multi-objective optimization is to convert multi-objective optimization into single-objective optimization through weighting factors. This method assigns different weights to each element during the election process and ideally ignores certain attributes after the synthesis operation. In addition, the deployment of relay nodes in the second stage adds additional overhead.

In these wireless sensor node deployment methods, either connectivity is guaranteed and coverage is ignored or the cost of the necessary number of deployed nodes is not considered. Studies have sought to improve deployment and connection coverage based on the required minimum number of nodes, but optimization algorithms based on the disk communication model and radio frequency propagation model cannot be used in underwater acoustic channels. Node deployment in WSNs is mostly used for 2D monitoring, and some applications require 3D monitoring, such as air pollution detection. Different from the spatial area deployment applications of WSNs, this article mainly focuses on the monitoring of target interest points in UWSNs.

2.2 Deployment of Specific Underwater Sensor Nodes

Underwater-specific sensor nodes are usually divided into three types: underwater processing nodes, underwater relay nodes, and surface gateway nodes. Alhumyani et al. [2] introduced an underwater processing node with stronger computing power than ordinary nodes to perform local processing on the collected data. The processing node deployment method reduced the end-to-end delay of UWSNs and extended the network lifetime. Zhang et al. [46] designed a 2D water surface gateway optimization deployment algorithm based on improved cuckoo search. The optimal deployment problem of water gateways is transformed from multi-objective optimization to single-objective optimization by weighting factors, and an improved cuckoo search algorithm is used to solve the optimal layout of multiple water gateways to achieve a fair and efficient distribution of water gateways. Liu et al. [28] studied the topic of adding relay nodes to a deployed UWSN to compensate for the defects of the original network topology. The surface sensor nodes are guided by a heuristic algorithm to sink to a suitable location to act as a communication relay between the nodes, thus achieving the goal of optimizing data routing in the network, balancing traffic distribution, and extending the network lifetime. Al-Salti et al. [1] designed a method for determining the water surface convergence node of an UWSN based on the center point division method. This method selects M nodes from the water surface candidate nodes as sink nodes through an iterative calculation method, to minimize the number of data transmission hops between the underwater sensor nodes and these sink nodes.

2.3 Deployments Involving All Underwater Sensor Nodes

Node deployments involving all underwater sensor nodes are typically divided into regional and event node deployments.

2.3.1 Regional Node Deployments. Senel et al. [35] used the connected dominance set method to find the optimal placement depth of nodes to maximize network coverage and ensure network connectivity. This method first classifies nodes into dominant and dominated; then the dominant calculates the depth of the dominated based on neighboring node information and sends the depth information to the dominated, which adjusts its depth to improve the coverage of the underwater area. Huang et al. [18] proposed a node placement algorithm based on a redundancy model and boundary effect. First, enough nodes are randomly deployed under the premise of expected quality. Then, the nodes judge whether they are redundant nodes—if they are, then they enter a dormant state; otherwise, the nodes use the virtual force algorithm to adjust their depth to improve network coverage. Khalfallah et al. [24] proposed a 3D underwater sensor deployment method based on sub-cubic subdivision of the monitoring area and mixed integer linear programming, which aims to minimize the deployment cost while ensuring the required quality of monitoring and connectivity. Jiang et al. [21] proposed a fully connected node deployment algorithm and a location scheduling algorithm. Nodes are deployed through a greedy iterative strategy to achieve larger coverage, then “connected nodes” are introduced to improve network connectivity, but the impact of the number of nodes was not considered.

Zhang et al. [48] proposed an optimal algorithm for 3D UWSN coverage enhancement based on an improved fruit-fly optimization algorithm. Jin et al. [22] proposed a deployment optimization mechanism using depth-adjustable nodes in UWSNs. The sink nodes are evenly distributed on the water surface as cluster heads. The sensor nodes in the cluster are adjusted vertically to form a topological structure with the sink node as the root node, so all nodes in the network are connected. Network deployment is optimized by finding the optimal location of nodes while keeping the network topology unchanged. Song et al. [37] proposed a node deployment scheme based on the evidence theory method. This scheme implements sonar probability perception and an enhanced

data fusion model to improve the prior probability deployment algorithm of Dempster–Shafer evidence theory and deploys fewer nodes to enhance network judgment standards and expand detection capabilities. Wang et al. [40] constructed an optimization model for the minimum number of sensor nodes required for a specific diverse k -coverage UWSN. In this model, a **k -equivalent radius enhanced virtual force algorithm (k -ERVFA)** is proposed to achieve an uneven regional coverage optimization for different k -coverage requirements. However, it minimizes the number of nodes under the premise of ensuring k -coverage but does not guarantee connectivity.

In these regional deployment methods, either network coverage is maximized at the expense of connectivity or connectivity is guaranteed without regard to the cost of the number of nodes deployed.

2.3.2 Event Node Deployments. Na et al. [30] proposed a fish-inspired algorithm for underwater sensor node placement. By simulating fish school behavior combined with congestion control, nodes can automatically trend and cover events while achieving node distribution density and event distribution. Wang et al. [41] proposed an optimization scheme for WSN deployment based on the optimized artificial fish swarming algorithm, which inherits the foraging and backward behavior of artificial fish in the algorithm and optimizes the ability to find the maximum objective function value. Du et al. [7] proposed a particle swarm-inspired algorithm for self-organized arrangement of underwater sensor nodes, which enables sensor nodes to autonomously converge and cover the target by simulating the movement behavior of particles in the search space and to match the node distribution density with the target distribution density. Combined with the dynamic simulation experiment results of the water flow field, this algorithm can achieve good performance when applied to the arrangement of underwater nodes and has the characteristics of distributed implementation, but network connectivity is not considered, and the scale of the tested nodes is small. Jiang et al. [20] proposed a wolf search-based redeployment algorithm for UWSNs (called RAWs), wherein the sensor nodes are uniformly distributed in the target area, and the nodes move toward the target when they sense an event and automatically escape when they encounter an obstacle. This algorithm imitates the wolf predator mechanism and combines congestion control to ensure the coverage of events and avoid falling into local optimality. The algorithm solves the problem of redeployment of nodes in UWSNs to a certain extent, but it does not consider network connectivity.

Arivudainambi et al. [3] used the cuckoo search algorithm to find the optimal location of nodes to achieve single coverage of a specific target in the underwater 3D space—that is, to ensure that the target is covered by at least one underwater sensor node. The cuckoo search algorithm is an emerging heuristic algorithm that uses the Levy flight mechanism to search for the optimal solution by simulating the parasitic brooding behavior of cuckoos. The underwater node arrangement scheme obtained by this algorithm outperforms random deployment and basically achieves full coverage of the target in the underwater 3D space; however, network connectivity is not considered. Su et al. [38] proposed a **Voronoi-based optimal depth adjustment (VODA)** deployment scheme, wherein gateway nodes collect coordinates of sensor nodes to build Voronoi diagrams. Certain sensor nodes are selected to remain on the water surface based on this diagram, called leader nodes. The remaining nodes need to be sunk to different depths to reduce coverage overlap between nodes. This approach improves coverage while ensuring connectivity, but the coverage achieved is ineffective and does not account for the reasonableness of the number of deployed nodes.

Among all node deployment methods, node deployment in WSNs is mostly used for 2D monitoring, although some applications require 3D monitoring; thus, most deployment methods cannot be directly applied to the underwater environment. Among all underwater node deployment

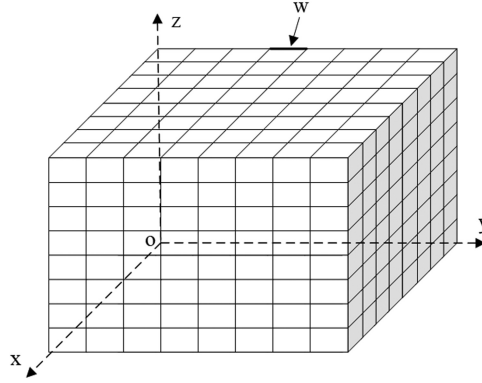


Fig. 1. Coordinate position of UWSNs.

methods, regional node deployments are relatively mature, whereas event node deployments research is relatively focused on maximizing coverage, ignoring network connectivity, or enhancing data transmission reliability and network robustness by increasing node density in the deployment area. The disadvantages of this approach are twofold: First, increasing the number of sensor nodes inevitably leads to higher hardware costs. Second, there is more overlap in the coverage area of nearby nodes, leading to the collection and transmission of redundant data, wasting valuable energy resources.

This article proposes a deployment method for target node monitoring in a 3D underwater environment. Different from the existing literature, this article constructs a model that maximizes network coverage and optimizes deployment cost while ensuring full connectivity. However, minimizing the number of deployed nodes may not be the optimal scheme. Under the premise of realizing full connectivity, we find the optimal number of nodes to deploy by selecting the maximum fuzzy operator value of target coverage and deployment number. According to the NP-hard property of the optimization model, an IMFO node deployment algorithm is proposed, and the fuzzy operator is cleverly used to achieve an optimal solution.

3 SYSTEM MODEL

In this section, we introduce the network scenario, describe the relevant performance metrics, and formulate the 3D UWSN deployment problem.

3.1 Network Scenario

We consider a 3D underwater network scenario with a size of $L \times W \times H$ and n sensor nodes randomly and uniformly distributed under the water. Let the set of sensors be $S = \{s_1, s_2, \dots, s_n\}$. The m event points are randomly and uniformly distributed underwater, and the set of event points is denoted as $T = \{t_1, t_2, \dots, t_m\}$. Figure 1 shows the target monitoring water area V with size $L \times W \times H$. The 3D underwater space can divide a large cube into several small cube areas, and the side length of each small cube is w . In the working process of the UWSN, sensor nodes below the water surface transmit information through acoustic communication. They transmit the collected information to the sink node through single- or multi-hop paths, and then the sink node transmits the information to the data center for analysis through satellite or ground-based stations. Each sensor has the ability of sensing, communication, and moving. Denote the attribute vector of s_k as $\mathbf{B}_k = \langle r_k, R_k, l_k, \mathbf{p}_k \rangle$, where $r_k \geq 0$, $R_k \geq 0$, describes the sensing radius and communication radius, respectively, and \mathbf{p}_k is the current position information sensed by s_k . All sensors in the

network have the same communication radius and sensing radius except the sink node, namely, $R_k = r^c, r_k = r^s (1 \leq k \leq n)$, and the communication radius is larger than the sensing radius. Nodes in the communication range of a node are called its neighbor nodes, and the node can perceive its location and the location of its neighbors. All wireless sensor nodes send and receive signals uniformly in all directions. The sensing range of the node is a spherical area with a circle as the center and a radius of r^s . Assume that the coordinates of any sensor node in the 3D underwater space is $\mathbf{p}_k = (x_k, y_k, z_k)$, and the coordinates of any monitoring event point m in the monitoring area is $\mathbf{p}_m = (x_m, y_m, z_m)$; then the Euclidean distance from the point to the sensor node can be put forward as:

$$d(\mathbf{p}_k, \mathbf{p}_m) = \sqrt{(x_m - x_k)^2 + (y_m - y_k)^2 + (z_m - z_k)^2}. \quad (1)$$

We denote the probability that the k th node senses event point m in the monitoring area as $f(\mathbf{p}_k, \mathbf{p}_m)$ [23], and its mathematical expression can be expressed as:

$$f(\mathbf{p}_k, \mathbf{p}_m) = \begin{cases} 0, & r^s + R_e \leq d(\mathbf{p}_k, \mathbf{p}_m) \\ e^{-\alpha\lambda}, & r^s - R_e < d(\mathbf{p}_k, \mathbf{p}_m) < r^s + R_e \\ 1, & d(\mathbf{p}_k, \mathbf{p}_m) \leq r^s - R_e, \end{cases} \quad (2)$$

where $\lambda = \lambda_1^{\beta_1} / \lambda_2^{\beta_2}$, $\lambda_1 = (R_e - r^s) + d(\mathbf{p}_k, \mathbf{p}_m)$, $\lambda_2 = (R_e + r^s) - d(\mathbf{p}_k, \mathbf{p}_m)$. α , β_1 , and β_2 are all attenuation coefficients of sensor nodes' ability to perceive things, and R_e denotes the uncertainty of sensor nodes' perception. For the space in the distance $r^s - R_e$, the node has a perception probability of 1, and for the distance outside $r^s + R_e$, the node has a perception probability of 0. The closer the node is to the target location, the more accurate the information collected. The farther away from the target, the more inaccurate the information.

3.2 Performance Metrics

Network coverage rate, network connectivity rate, and number of deployed nodes are three important metrics of the performance of UWSN node deployments, which are described here in detail.

3.2.1 Network Coverage Rate. The network coverage rate is used to describe the size of the network's ability to monitor the target area. The larger the network coverage rate, the more comprehensive the sensor network's monitoring of the target event point. Assume that there are n sensor nodes s_1, s_2, \dots, s_n in the network and the coverage of point p is, respectively, $c_p(s_1), c_p(s_2), c_p(s_3), \dots, c_p(s_n)$; then the coverage of point p in the network is denoted as:

$$c_p(Sov) = 1 - \prod_{i=1}^n (1 - c_p(s_i)). \quad (3)$$

To better detect the target event points in the network, the coverage rates of m event points in the network are averaged to obtain the overall coverage of the network as:

$$C_{cov} = \frac{1}{m} \sum_{i=1}^m c_p(Sov). \quad (4)$$

3.2.2 Network Connectivity Rate. Collaborative work between nodes that enables target monitoring can only be accomplished if the nodes are interconnected. The greater the network connectivity rate, the better the connectivity of the sensor network. After the sensor node collects the target event point information, it transmits the collected information to the surface sink node through a single-hop or multi-hop path. The network connectivity rate is defined as the ratio of

the number of nodes N_{nec} connected to a sink node by a single- or multi-hop path to the total number of nodes n , denoted as $C_{\text{nec}} = N_{\text{nec}}/n$.

3.2.3 Number of Sensor Nodes Deployed. As sensors are deployed, they cannot be recharged underwater and fail once they run out of power; thus, increasing the number of sensor nodes will inevitably lead to higher hardware costs. Therefore, the number of deployments is positively related to the cost.

3.3 Problem Description

The sensor's ability to sense event points obeys the perception probability model, wherein high coverage performance is achieved with as few sensor nodes as possible while ensuring connectivity. This problem is described as:

$$\begin{aligned}
 (C_{\text{cov}}^*, n^*) &= \text{argmax } F(C_{\text{cov}}, n) \\
 \text{Subject to :} \\
 C_1 : C_{\text{cov}} &= \frac{1}{m} \sum_{i=1}^m c_p(\text{Sov}) \\
 C_2 : \sum_{(i,j) \in E} x_{ij} - \sum_{(i,j) \in E} x_{ji} &\geq 1, \forall (i,j) \in E, j \neq \text{sink} \\
 C_3 : x_{ij} &\geq 0 \\
 C_4 : n &\in [N_s, N_e],
 \end{aligned} \tag{5}$$

where the F function represents the objective function given C_{cov} and n , which means that the optimal number of sensor nodes n^* is deployed while maximizing the overall coverage of the network C_{cov}^* under the constraints. C_1 is the expression for the overall network coverage rate, $E = \{(i,j) \in n : i \neq j, d(i,j) \leq R_k\}$. x_{ij} is the traffic load from node i to node j , and C_2 indicates that there is at least one path between any two sensor nodes deployed to transmit data packets—that is, full connectivity is guaranteed. C_3 indicates that the number of transmitted data packets must be greater than or equal to 0. C_4 indicates that the number of nodes is within the acceptable size for the user to deploy sensors, with a minimum number of N_s and a maximum number of N_e . Such monitoring problems are mixed integer linear programming problems, which have been shown to be NP-hard problems [26].

4 Design of IMF²O²

In this section, we describe in details the proposed IMF²O² algorithm, including the fully connected node deployment algorithm with a fixed number of nodes, an objective function design based on fuzzy operators, and the process description of the IMF²O² algorithm. To describe the IMF²O² algorithm more intuitively, we provide a diagram of the algorithm's structure at the end of this section.

4.1 Fully Connected Node Deployment Algorithm with Fixed Number of Nodes

4.1.1 Fitness Function Design Based on Fuzzy Operator. Most objective optimizations in existing node deployment schemes only consider the single objective of maximizing network coverage, ignoring the importance of network connectivity to node deployment. The method for multi-objective optimization is to convert multi-objective optimization into single-objective optimization through weighting factors. This method assigns different weights to each element during the election process and ideally ignores certain attributes after the synthesis operation. To solve this problem, this article introduces the concept of the fuzzy operator in fuzzy theoretical

mathematics. Considering network coverage and network connectivity, the suitable membership function of the target quantity is selected as the fuzzy operator, and each target quantity is calculated and fused according to the fuzzy operator formula to achieve the balance of advantages among the influence of each target quantity.

Definition 4.1. Let \tilde{A} be a map from domain X to $[0,1]$, that is:

$$\tilde{A}: X \rightarrow [0, 1], x \rightarrow A(x), \quad (6)$$

where \tilde{A} is called a fuzzy set on X , the $\tilde{A}(\cdot)$ function is the membership function of the fuzzy set \tilde{A} , and $\tilde{A}(x)$ is the membership degree of x to the fuzzy set \tilde{A} .

According to the properties of fuzzy operators [17], the value range of the two parameters of coordinated fusion is between 0 and 1. As noted in Section 3.2, the values for both network coverage and network connectivity are in between 0 and 1 and do not require normalization. According to the characteristics of network coverage and network connectivity rate, the ascending half-Cauchy was chosen as the membership function, given as:

$$y_1 = y_2 = \begin{cases} v, & 0 < x < \tau \\ \frac{1}{1+\tau(x-\tau)^{-\sigma}}, & \sigma \leq x < 1, \end{cases} \quad (7)$$

where y_1 and y_2 are the membership functions for network connectivity and network coverage, respectively, and the independent variable x in this equation represents the network connectivity or network coverage rate. τ , σ , and v are constants that can be set according to specific needs. Commonly used values are $\tau = 0.1$, $\sigma = 3$ and $v = 0.01$. When the node network coverage or network connectivity rate is below 0.1, it can be regarded as poor network coverage or network connectivity, and the membership degree of the network coverage or network connectivity rate at this time is defined as 0.01. When the value is higher than 0.1 and lower than 0.3, the network coverage or network connectivity rate is considered to be average. When the value is higher than 0.4, its membership value increases rapidly with the increase of network coverage or network connectivity, which greatly increases the probability of its selection.

Deploying underwater sensors is costly, and the fewer required to achieve the same performance, the better. Depending on the deployment, the number of nodes is used as a parameter for normalization, which can be expressed as:

$$\varphi_n = n/N_n, \quad (8)$$

where n is the current number of deployments, N_n is the number in the set of sensor nodes, and φ_n denotes the value normalized to the number of deployed nodes. Based on the relationship between the number of deployments and the cost, a Gaussian membership function is chosen to calculate its membership given by:

$$y_3 = e^{-k \frac{(x-c)^2}{2\sigma}} - 1/2, \quad (9)$$

where c and σ are the expected value and standard deviation of the function, which determine the position and shape of the change in the function, respectively. Because the number of deployments is inversely proportional to the probability of selection, it is a small function and takes $c = 0$. In addition, the number of deployments is normalized to take values in the range (0, 1), taking $\sigma = 1$ and $k = 2$.

The fuzzy operator is derived from fuzzy mathematics, and its mathematical expression is:

$$f\{\pi(i), \dots, \pi(k)\} = \frac{\prod_{i=1}^k \pi(i)}{1 - \sum_{i=1}^k \pi(i) + \sum_{i \neq j} (\pi(i) \cdot \pi(j))}, \quad (10)$$

where $\pi(i) \in [0,1]$, k is the number of unknown parameters, and the operator satisfies the following properties:

- (1) Similar information has reinforcing properties, namely, $f\{\pi(i), \dots, \pi(k)\} \geq \max\{\pi(i), \dots, \pi(k)\}$, $\pi(i) \geq 0.5, \dots, \pi(k) \geq 0.5$, or $f\{\pi(i), \dots, \pi(k)\} \leq \min\{\pi(i), \dots, \pi(k)\}$, $\pi(i) \leq 0.5, \dots, \pi(k) \leq 0.5$.
- (2) Heterogeneous information is harmonious—that is, $\min\{\pi(i), \dots, \pi(k)\} < f\{\pi(i), \dots, \pi(k)\} < \max\{\pi(i), \dots, \pi(k)\}$ and $\prod_{i=1}^k \pi(i) < 0$.

The introduction of the fuzzy operator enhances the probability of target selection for network coverage and network connectivity in this group of node deployments; e.g., if both network coverage and network connectivity are in good condition and the membership degree is greater than 0.5, then the probability of selection for this group of node deployments increases. Similarly, fuzzy operators can also weaken the interference of contradictory information elements, such as network coverage and deployment cost. Increasing the number of deployed sensors will improve network coverage but also increase the cost of deployment. In summary, a multi-objective optimization model using fuzzy operators can be expressed as follows:

$$\begin{aligned} & \max f(y_1, y_2) \\ & \text{s.t.} \begin{cases} C_5 : y_1, y_2 \in (0, 1) \\ C_6 : (x_i, y_i, z_i) \in V, \forall i \in n \end{cases}, \end{aligned} \quad (11)$$

where $f(y_1, y_2)$ denotes the node deployment scheme selected by considering the size of the membership function of the network coverage and network connectivity together. Constraint C_5 indicates that the values of network coverage and network connectivity are between 0 and 1. (x_i, y_i, z_i) denotes the 3D coordinate position of the i th node, and constraint C_6 is that the node must always be in the target area V .

4.1.2 Improved Moth Flame Optimization Algorithm. Moth-flame optimization (MFO) [29] algorithm proposed by Mirjalili, an Australian scholar, is a new biological heuristic algorithm. The traditional MFO algorithm is a novel swarm intelligence optimization algorithm with simple structure and fewer parameters than other similar algorithms. Therefore, it has been studied and applied by many scholars since it was proposed. Although the traditional MFO algorithm has these advantages, it also has slow and premature convergence. The spiral flight search of the traditional MFO algorithm has a better local search capability and coverage search level for the target area. However, after a certain number of iterations, the spiral flight search will have a smaller update phenomenon, which makes the algorithm converge slower in the late iteration. When the traditional MFO algorithm finds the local optimal solution, the moths gather near the local optimal solution, which leads the algorithm to fall into the local optimal area and premature convergence.

Based on the shortcomings of slow and premature convergence of the traditional MFO algorithm, this article proposes an **improved moth-flame optimization (IMFO)** algorithm. In view of the slow convergence speed of the traditional MFO algorithm, this article adopts the moth position update formula of the traditional MFO algorithm to speed up convergence and assigns weights to the best flame and the j th flame. As the number of iterations increases, the greater the weight of the global optimal flame at the later stages of the iteration. l_{curr} denotes the current number of iterations, l_{max} denotes the maximum number of iterations, and F_{best} is the optimal flame. The improved update formula of the i th moth position M_i is:

$$M_i = D_i \cdot e^{bt} \cdot \cos(2\pi t) + \frac{l_{\text{curr}}}{l_{\text{max}}} F_{\text{best}} + \left(1 - \frac{l_{\text{curr}}}{l_{\text{max}}}\right) F_j. \quad (12)$$

ALGORITHM 1: IMFO Algorithm

```

—  $n$ : number of nodes
—  $m$ : number of target monitoring points
—  $l_{\max}$ : maximum number of iterations
Require: Initial  $n$ ,  $m$  and  $l_{\max}$  value
Ensure: The coordinate position of the node
1: Initialize all parameters
2: the fitness function in this algorithm is calculated using Equation (11)
3: perturbation = false, count = 0
4: while  $l_{\text{curr}} < l_{\max} + 1$  do
5:   if  $l_{\text{curr}} == 1$  then
6:     sort the initialized moths according to the fitness
7:     update flame
8:   else if ! perturbation then
9:     integrate and sort the optimal moth with the flame
10:    update flame
11:   else
12:     perturbation = false
13:     perform mutation operation
14:     update the flame position
15:   end if
16:   if  $F_{\text{best}}$  has not been improved then
17:     count = count + 1
18:   else
19:     count = 0
20:   end if
21:   if count  $\geq x$  then
22:     perturbation = true
23:     count = 0
24:   end if
25:   if ! perturbation then
26:     for (all moths in current population) do
27:       Update the moth position by Equation (12)
28:     end for
29:   end if
30: end while

```

The traditional MFO algorithm suffers from premature convergence, and this article takes inspiration from the literature [16] and adopts the method of not falling into local optimum. If x consecutive iterations do not improve the current global solution, then such an iteration is considered an iteration failure. When x consecutive iterations fail, then the currently checked solution is expected to contain some local minima. Once such a possible local minimum appears, a perturbation mechanism is employed to find a better domain in the search space.

As important research content of genetic algorithms, the mutation operator plays the role of changing some gene values of individual strings in the population. There are two purposes for introducing mutation: (a) When the algorithm is close to the optimal solution field, the local random search ability of mutation operator can be used to accelerate the convergence to the optimal solution; and (b) to maintain population diversity prevent premature convergence. The IMFO-based deployment algorithm for underwater sensor nodes is described as Algorithm 1.

Step 2 is to indicate that the fitness function of Algorithm 1 is calculated by Equation (11). Step 3 is to set the initial flag of the perturbation mechanism, Steps 12 to 15 are the perturbation mechanism of the mutation operator, Steps 21 to 24 are the judgment conditions for the implementation of the perturbation mechanism, and Steps 25 to 29 are the globally optimal flames to replace the j th flame corresponding to the moth, which maintains the optimal position solution for the flame. The perturbation mechanism of the selection variation operator in Algorithm 1 maintains the diversity of the population and does not replace the original MFO algorithm.

4.1.3 Time Complexity Analysis of IMFO Compared to MFO. Compared with the traditional MFO algorithm, the IMFO algorithm uses the global optimal flame to replace the j th flame corresponding to the moth without increasing the time complexity, and the time complexity after introducing the mutation operator:

$$\begin{aligned} T_{\text{IMFO}} &= (1 - p) \cdot T_{\text{MFO}} + p \cdot T \cdot T_{\text{Muta}} \\ &= O(T(N^2 + ND)), \end{aligned} \quad (13)$$

where p is 1 if a perturbation step is performed and p is 0 otherwise, T is the maximum number of iterations, T_{Muta} is the time complexity of mutation, D is the problem dimension, and N is the number of moths. The time complexity of the IMFO algorithm is $O(N^2)$ in the worst case and $O(N \times D)$ for updating the moth's position. When the perturbation step is executed, the step of the spiral position update of the MFO algorithm is suspended. Adding a perturbation step only increases the number of evaluations of the cost function and does not increase the additional computational complexity of the spiral position update of the MFO algorithm, so the time complexity of introducing the mutation operator perturbation mechanism is almost unchanged.

4.2 Objective Function Design Based on Fuzzy Operator

Definition 4.2. Let $\tilde{A} \in \zeta(X)$, if $\forall x_1, x_2 \in X, \forall \lambda \in [0, 1]$; thus, we have:

$$\tilde{A}(\lambda x_1 + (1 - \lambda) x_2) \geq \tilde{A}(x_1) \bigwedge \tilde{A}(x_2). \quad (14)$$

This is called a convex fuzzy set.

Definition 4.3. Let $\tilde{A} \in L_2^E$ be a 2D convex fuzzy set, $A(x) = (A^1(x) A^2(x))$, for $\lambda \in [0, 1]$, let

$$A_\lambda(x) = \begin{cases} 1, & A^1(x) \geq \lambda \\ 1/2, & A^1(x) < \lambda \leq A^2(x) \\ 0, & \lambda > A^2(x) \end{cases}, \quad (15)$$

then A_λ is called the λ cut set of \tilde{A} [49].

After the network is fully connected, network coverage increases with the number of nodes deployed, but when the number increases to a certain amount, there is more overlap in the coverage area of nearby nodes, resulting in slower coverage growth and also increased deployment costs. $f(y_2, y_3)$ is a 2D convex fuzzy set (see Proposition 1 for the proof). The fuzzy operator is used to comprehensively consider the network coverage and deployment cost. The maximum value of the membership function is the optimal deployment scheme, and its objective optimization model is formulated as:

$$\begin{aligned} &\max f(y_2, y_3) \\ &s.t. \begin{cases} C_5 : y_2, y_3 \in (0, 1) \\ C_6 : (x_i, y_i, z_i) \in V, \forall i \in n \end{cases}, \end{aligned} \quad (16)$$

where y_2 is the coverage rate, y_3 is the normalized value of the number of nodes, and $f(y_2, y_3)$ denotes the deployment scheme selected by comprehensively considering the network coverage

rate and the membership degree of the number of deployed nodes. (x_i, y_i, z_i) denotes the 3D coordinate position of the i th node, and C_6 holds that the node must always be in the target area V .

PROPOSITION 1. $f(y_2, y_3)$ is a 2D convex fuzzy set, which can obtain a unique maximum value in its range of values.

PROOF. First prove that $\tilde{A} \in L_2^E$ is a 2D convex fuzzy set if and only if \tilde{A}^1 and \tilde{A}^2 are convex fuzzy subsets on E (condition to be demonstrated).

First, prove the necessity of these conditions to be demonstrated: According to Definition 4.2, for any $x_1, x_2 \in E$ and $\alpha \in [0, 1]$, there is $A_\lambda((1-\alpha)x_1 + \alpha x_2) \geq A_\lambda(x_1) \wedge A_\lambda(x_2)$. If $A_\lambda(x_1) \wedge A_\lambda(x_2) = 1$, then $A^1(x_1) \geq \lambda, A^1(x_2) \geq \lambda$. Since A^1 is a convex fuzzy subset on E , then $A^1((1-\alpha)x_1 + \alpha x_2) \geq A^1(x_1) \wedge A^1(x_2) \geq \lambda, A_\lambda((1-\alpha)x_1 + \alpha x_2) = 1$. If $A_\lambda((1-\alpha)x_1 + \alpha x_2) = 1/2$, then $A^2(x_1) \geq \lambda, A^2(x_2) \geq \lambda$. Because A^2 is a convex fuzzy subset on E , $A^2((1-\alpha)x_1 + \alpha x_2) \geq A^2(x_1) \wedge A^2(x_2) \geq \lambda, A_\lambda((1-\alpha)x_1 + \alpha x_2) \geq 1/2 = A_\lambda(x_1) \wedge A_\lambda(x_2)$. Thus, for any $x_1, x_2 \in E$ and $\alpha \in [0, 1]$, we have $A_\lambda((1-\alpha)x_1 + \alpha x_2) \geq A_\lambda(x_1) \wedge A_\lambda(x_2)$.

Proof of sufficiency: For the hypothesis $\exists 1 \leq i \leq 2$ such that A^i is not a convex fuzzy subset on E , there exist $x_1, x_2 \in E$ and $\alpha \in [0, 1]$ such that $A^i((1-\alpha)x_1 + \alpha x_2) < A^i(x_1) \wedge A^i(x_2)$. $\exists \lambda \in (0, 1)$, such that $A^i((1-\alpha)x_1 + \alpha x_2) < \lambda < A^i(x_1) \wedge A^i(x_2)$, then $A^i(x_1) > \lambda, A^i(x_2) > \lambda$, so $A_\lambda(x_1) \geq (3-i)/2, A_\lambda(x_2) \geq (3-i)/2$. Also, because \tilde{A} is a 2D convex fuzzy set, there is $A_\lambda((1-\alpha)x_1 + \alpha x_2) \geq A_\lambda(x_1) \wedge A_\lambda(x_2) \geq (3-i)/2$, which shows that $A^i((1-\alpha)x_1 + \alpha x_2) \geq \lambda$ contradicts.

In summary, $f(y_2, y_3)$ can be proved to be a 2D convex fuzzy set once it is shown that both y_2 and y_3 in $f(y_2, y_3)$ are convex fuzzy subsets. Because the membership function image of y_2 is monotonically increasing, it follows from Definition 4.2 that y_2 is a convex fuzzy set, the membership function image of y_3 is monotonically decreasing, which is also a convex fuzzy set. Therefore, it can be proved that $f(y_2, y_3)$ is a 2D convex fuzzy set. \square

4.3 IMF²O² Algorithm

Combined with the node deployment algorithm with a fixed number of nodes in Section 4.1, an **Improved Moth Flame Optimization Algorithm Based on Fuzzy Operator (IMF²O²)** is proposed. Because the optimization model in this article seeks to achieve high coverage performance with as few sensor nodes as possible with full connectivity, the small number of nodes and high coverage are two opposing performance metrics. From a mathematical point of view, one equation cannot solve two unknowns at the same time. Therefore, the IMF²O² algorithm starts by generating a random number of nodes from a range of user-acceptable nodes to find the network coverage and iterates until the most appropriate number of nodes is selected. The node deployment algorithm based on IMF²O² is described as Algorithm 2.

Step 3 is to randomly initialize a number of deployment nodes, i is the number of currently selected sensor nodes. Steps 5 to 8 are the deployment process of the IMFO algorithm with Equation (11) as the fitness function, which aims to maximize the coverage while ensuring a connectivity of 1. Steps 9 to 24 use the gradient search method with maximizing Equation (16) as the objective function to obtain the maximum coverage rate and the optimal number of deployed nodes. If the fitness value calculated by the next number of nodes is larger than the current value, then it means that it is on the upward trend of the convex fuzzy set curve and the number of nodes should continue to increase to find the maximum number of nodes. If the fitness value calculated by the next number of nodes is smaller than the current value, then it indicates the downward trend of the convex fuzzy set curve and the number of nodes should be reduced to find the maximum number of nodes, corresponding to Steps 19 to 21. If the fitness value is decreasing when it increases to a

ALGORITHM 2: IMF²O² Algorithm

- $[N_s, N_e]$: range of sensor numbers
- $L \times W \times H$: monitoring area size
- w : side length of the sub-cube
- N_{opt} : optimal number of sensors
- C_{cov} : network coverage
- C_{nec} : network connectivity

Require: Initial w , $[N_s, N_e]$ and $L \times W \times H$ value

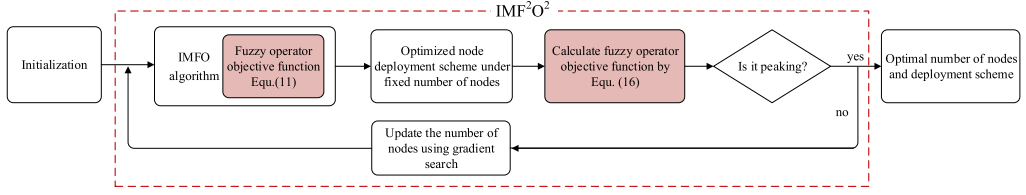
Ensure: N_{opt} , C_{cov} and C_{nec}

- 1: Calculate the size and coordinates of the target monitoring point according to the size of $L \times W \times H$ and w
- 2: $(N_{\text{opt}}, F_{\text{max}}) = (0, 0)$
- 3: $i = \text{random}(N_s, N_e)$
- 4: **while** $i \in (N_s, N_e)$ **do**
- 5: **while** $C_{\text{nec}} \neq 1$ **do**
- 6: Calculate the objective function using Equation (11)
- 7: Run the IMFO algorithm to calculate C_{cov} and C_{nec} ;
- 8: **end while**
- 9: Calculate F_i using Equation (16) with $C_{\text{cov}}(i)$ and i as input variables.
- 10: **if** $F_{\text{max}} < F_i$ **then**
- 11: $N_{\text{opt}} = i$
- 12: $F_{\text{max}} = F_i$
- 13: **if** $i > N_{\text{opt}}$ **then**
- 14: $i = i + 1$
- 15: **else**
- 16: $i = i - 1$
- 17: **end if**
- 18: **else**
- 19: **if** $i > N_{\text{opt}}$ **then**
- 20: $i = i - 2$
- 21: **else**
- 22: break
- 23: **end if**
- 24: **end if**
- 25: **end while**
- 26: $C_{\text{cov}} \leftarrow F_{\text{max}}$
- 27: **return** N_{opt} , C_{cov} and C_{nec}

certain number, then it means that a peak has been reached and the cycle is ended at this time, corresponding to Steps 21 to 23. If the process of reducing the number shows that the fitness value first increases and then decreases, then it means that a peak has been reached and at this time, the loop ends. Algorithm 2 structure is shown in Figure 2.

PROPOSITION 2. *The IMF²O² algorithm makes the network connectivity rate always 1 during the node deployment iteration process.*

PROOF. It can be deduced from the fuzzy operator Equation (10): $f(y_1, y_2) = \frac{y_1 \cdot y_2}{y_1 \cdot y_2 + (1 - y_1)(1 - y_2)}$, $y_1, y_2 \in (0, 1)$. When the values of y_1 and y_2 are close to 1, the value of $(\frac{1}{y_1} - 1)(\frac{1}{y_2} - 1)$ is the smallest—that is, the closer the membership degree of the network connectivity rate and network coverage rate is to 1, the greater the value of $f(y_1, y_2)$, close to 1. Because the fuzzy operator has the same information reinforcement and heterogeneous information harmony, only when y_1

Fig. 2. IMF²O² algorithm structure.

and y_2 are greater than 0.5 can $f(y_1, y_2)$ achieve the maximum value. Full coverage cannot be achieved with a smaller number of sensors, but it is possible to maintain full connectivity. Taking $f(y_1, y_2)$ as the fitness function to improve connectivity and network coverage using the IMFO algorithm, when the connectivity is 1 and the connectivity membership value is 0.9, the scheme with the largest corresponding coverage membership value is saved as the optimal scheme until the next value with a connectivity of 1, and a value with a larger coverage rate membership value replaces the previous optimal scheme. Therefore, using the IMF²O² algorithm can maintain full connectivity, and the proof is completed. \square

Because sensor perception of event points obeys a perceptual probability model and the location of the target monitoring point cannot be known in advance, to improve the coverage of event points, the monitored waters are divided into sub-cubes, each of which is considered as an event point to improve the overall coverage of the monitored waters. Assume that point p is at the center of the divided sub-cubes, and the coverage of point p in the network is denoted as $c_p(Sov)$; see Equation (3). The size of the target monitoring area is $L \times W \times H$, and the side length of each small cube is w , which is divided into $N_{\text{area}} = (L \times W \times H) / w^3$ sub-cubes in total. We can calculate the coverage of all sub-cube points divided by:

$$C_{\text{cov}} = \frac{1}{N_{\text{area}}} \cdot \sum_{x=1}^{L/w} \sum_{y=1}^{W/w} \sum_{z=1}^{H/w} c_p(Sov). \quad (17)$$

The computational complexity of the overall coverage is $O(N_{\text{area}} \times n)$, and the total number of sub-cubes divided is inversely proportional to w^3 . The smaller w is, the more the monitoring area is divided into sub-cubes, and the more possibilities for finding a better deployment solution, achieving more effective coverage and connectivity. At the same time, the space complexity of the algorithm will increase, so the value of w needs to be selected according to the specific quantity scale and experimental experience. The value of w in this article is based on experimental experience—that is, a value that greatly reduces the complexity and provides more options for the solution is selected according to the experimental situation.

5 SIMULATION AND PERFORMANCE EVALUATION

In this section, to verify the performance of the scheme proposed IMF²O², simulation experiments are carried out on the MATLAB R2018b platform. Sensor nodes are deployed for a $120\text{m} \times 120\text{m} \times 120\text{m}$ sea area, with monitoring event points randomly and uniformly distributed throughout the underwater environment. For the analysis of the size of the parameter w , a value $w = 10$ was chosen based on the experimental situation, accounting for the complexity of the calculation and performance, which significantly reduces the complexity and has a low impact on the accuracy. To facilitate the calculation of the network connectivity rate, it is assumed that the sink nodes are randomly distributed in the water surface area and the sensor nodes are connected to

Table 1. Parameter Settings

Parameter	Value
Number of nodes	6 ~ 16
Number of sinks	2
Number of monitoring points	50 ~ 200
Sense range r^s	35
Communication range r^c	60
Uncertainty factor R_e	8
Consecutive failed iterations x	5
Attenuation factor $\alpha/\beta_1/\beta_2$	0.8/1/1.5
Constants τ/σ	0.1/3
Population	20
Mutations rate	0.3
Maximum iterations	30

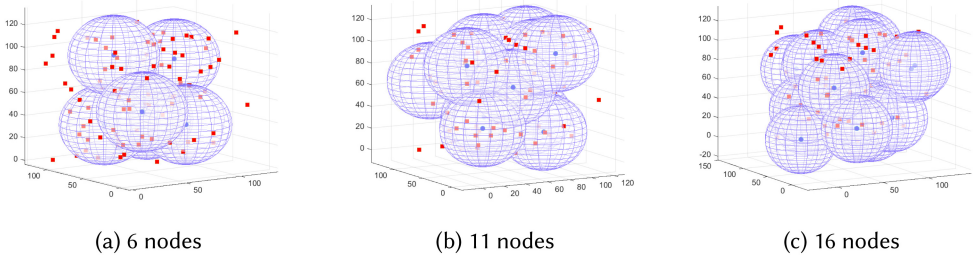


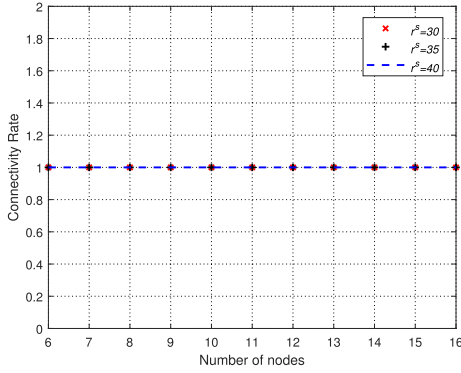
Fig. 3. 3D visualization of deployment with different number of nodes.

the sink node through one or more hops. The parameter settings for the experimental simulations are shown in Table 1.

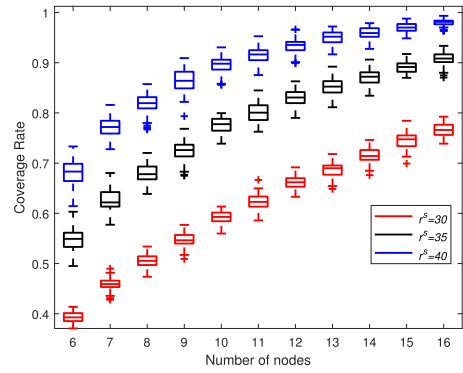
5.1 Impact of Parameters

As shown in Figure 3, the IMF²O² scheme is displayed in 3D visualization. Figures 3(a), 3(b), and 3(c) show the deployment of 6, 11, and 16 nodes to 200 target monitoring points, respectively. The blue dots represent sensor nodes, the red squares represent target monitoring points, and the purple sphere coverage represents the sensing coverage of sensor nodes. Figure 3(a) has the lowest number of nodes, a higher number of uncovered monitoring points, and a lower coverage rate; Figure 3(b) has a higher coverage rate; and Figure 3(c) has the best coverage and most overlapping coverage areas. The more sensor nodes, the better the coverage and the greater the overlap of the coverage area.

Based on the parameters in Table 1, parameter comparison experiments are conducted for the IMF²O² deployment scheme, each repeated 100 times to ensure objectivity. Experimental results are represented using boxplots showing five quantities: the lower quartile 25%, the median, the upper quartile 75%, and the two extreme observations. Figure 4 shows a simulation diagram of the network coverage and network connectivity rate achieved by a group of IMF²O² schemes with different sensing ranges when the communication radius is 60. Figure 4(a) portrays the change of the network connectivity rate with the number of deployed nodes under different sensing ranges. As the number of deployed nodes increases, the network connectivity rate is always 1, which indicates that the proposed IMF²O² can ensure full network connectivity. Figure 4(b) depicts that

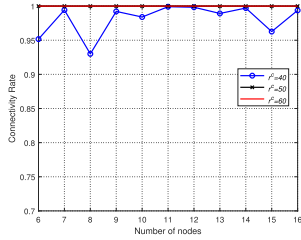


(a) Network connectivity rate varies with the number of nodes

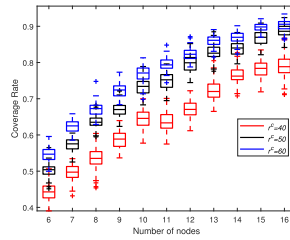


(b) Network coverage rate varies with the number of nodes

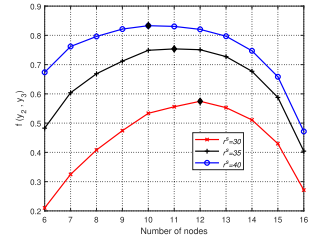
Fig. 4. Network coverage and network connectivity under different sensing radii.



(a) Network connectivity rate



(b) Network connectivity rate



(c) $f(y_2, y_3)$ changes with the number of nodes

Fig. 5. Example of determining the optimal number of nodes.

the larger the sensing range, the larger the network coverage. As the number of deployed nodes increases, the network coverage also increases, but with the increase in nodes, the growth rate of coverage gradually slows, indicating that the overlapping area between nodes increases.

Figure 5 shows an example of getting the optimal number of nodes for a sensing range of 35 and different communication ranges. Figure 5(a) depicts when the communication range is 50 or 60, the network is fully connected; when the communication range is 40, the network connectivity rate can reach more than 95% even when the number of nodes is small, indicating that IMF²O² is very effective in ensuring full network connectivity. Figure 5(b) portrays the change of the network connectivity rate with the number of deployed nodes under different communication ranges. The larger the communication range, the greater the network coverage achieved. IMF²O² uses a multi-objective selection mechanism based on fuzzy operators to maximize the coverage and connectivity as a fitness function. The larger the communication range, the easier it is to achieve a fully connected deployment, at which point the solution with the greatest coverage is selected, given full connectivity. When the communication range is small, the algorithm sacrifices network coverage in exchange for high connectivity. The objective of this research is to achieve high coverage performance at a lower cost while achieving full connectivity; therefore, the performance metrics of deployment cost and coverage are comprehensively considered. Figure 5(c) is a graph that shows the relationship between $f(y_2, y_3)$ and the number of nodes under different sensing ranges, wherein the black diamond block points indicate the maximum points in that curve segment. We can see that $f(y_2, y_3)$ first rises and then falls as the number of nodes increase. $f(y_2, y_3)$

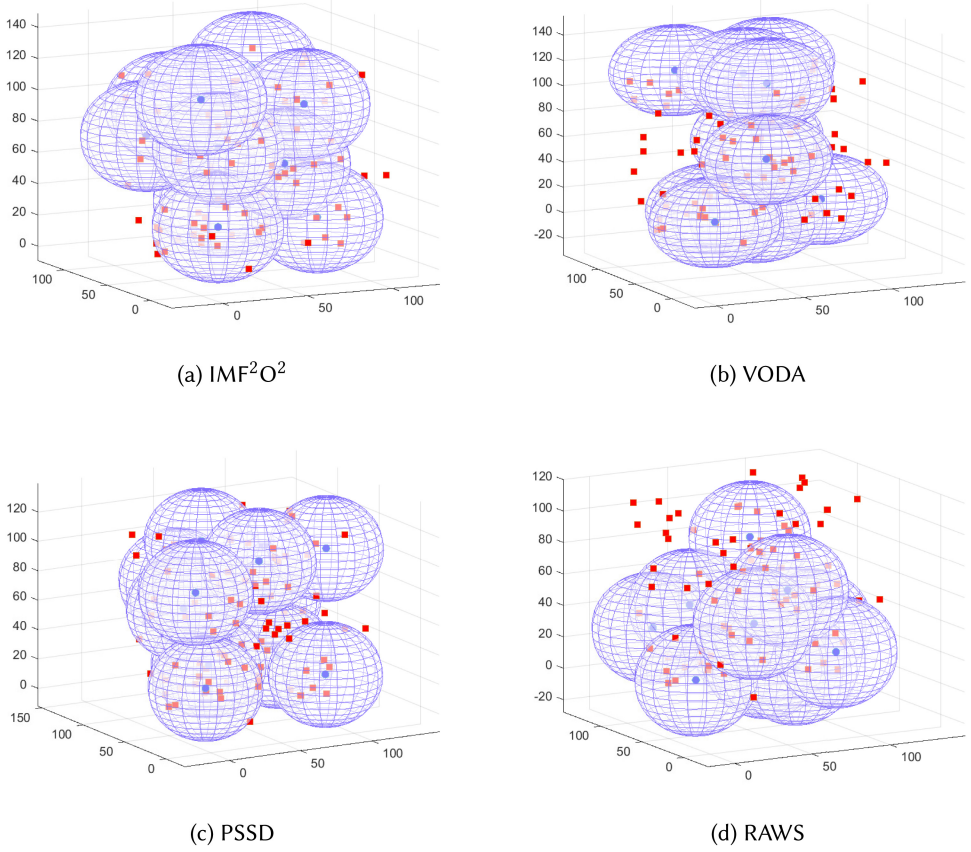


Fig. 6. Experimental results comparing the method of this article with related methods.

is a 2D convex fuzzy set that must have maximum points in its region, as proved in Proposition 1. Different sensing ranges correspond to different optimal number of nodes for deployment. Taking the sensing radius 35 as an example, the value of $f(y_2, y_3)$ is maximized when the number of deployed nodes is 11. At this time, 11 is the optimal number of deployed nodes.

5.2 Performance Comparison

We compare the performance of the IMF²O² to the PSSD [7], RAWs [20], VODA [38], and random node deployment schemes. PSSD and RAWs are both bio-inspired intelligent optimization algorithms, and the VODA scheme seeks to reduce coverage overlap while ensuring full connectivity. The PSSD scheme is set with a weight $\omega = 0.72$, a learning factor $c_1 = 1.49$, $c_2 = 1.49$, and a maximum particle movement speed $V_{max} = 30$. Figure 6 depicts the 3D visualization of the target monitoring of four schemes: IMF²O², VODA, PSSD, and RAWs. The blue dots in the figure represent sensor nodes, the red squares indicate target monitoring points, and the purple sphere coverage represents the sensing coverage of sensor nodes. The number of sensor deployments is set to 11, and 100 target monitoring nodes are randomly and evenly distributed underwater. Figure 6(a) shows the deployment of nodes in the IMF²O² scheme is relatively concentrated, which is to ensure full connectivity, and the number of monitoring points not covered is small, indicating a high level of network coverage. Figures 6(b) and 6(c) show that the number of uncovered monitoring

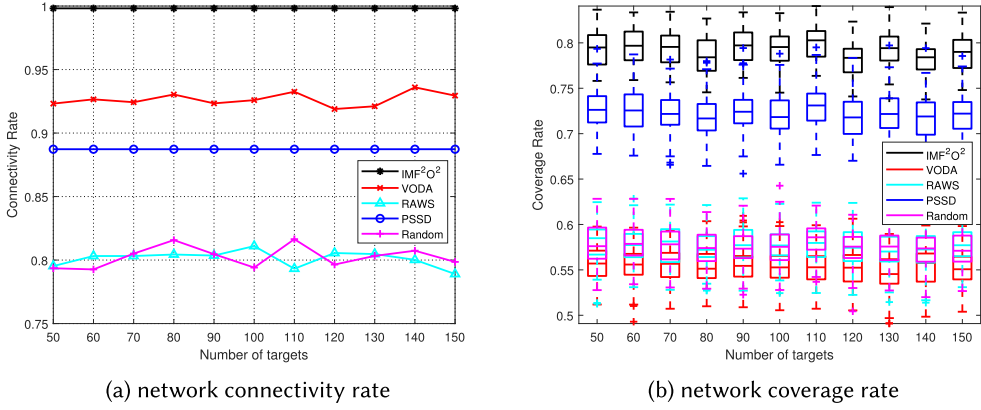


Fig. 7. Performance comparison of five methods.

points in VODA and PSSD are relatively large. The RAWs scheme in Figure 6(d) has a more diffuse deployment, the connectivity is the lowest, a high number of monitoring points are uncovered, and it has the least effective coverage.

We tested UWSNs consisting of 11 sensors with 50 to 150 target monitoring points randomly placed. To ensure the objectivity of the experiment, the experiment of proposed scheme was repeated 100 times to obtain the mean value, and the random deployment experiment of the target monitoring point was repeated 20 times to obtain the mean value. Figure 7 shows the five schemes of IMF²O², VODA, PSSD, RAWs, and random as simulated and compared under the same conditions. Figure 7(a) portrays the relationship between the network connectivity rate and the target number of monitoring points achieved by different node deployment schemes. The connectivity rate achieved by IMF²O² is 1—that is, full connectivity is achieved. Full connectivity under VODA is theoretically possible but requires a high number of gateway deployments and connectivity to common nodes randomly distributed on the level. Because the experiments in this article set up two gateways randomly distributed on the level, the connectivity rate of VODA is 0.92. The network coverage of the PSSD scheme is about 0.88, and the fitness function of the PSSD scheme only considers the network coverage and does not consider the network connectivity rate. Because the fitness function in the RAWs node deployment scheme only considers network coverage, and node movement tends to favor neighbor nodes with monitored event points, making nodes bunch up and resulting in a low network connectivity rate of about 0.8. IMF²O² improved the network connectivity rate by 12%, 20%, and 8% as compared to PSSD, RAWs, and VODA, respectively. Figure 7(b) depicts the relationship between the network coverage rate and the target number of monitoring points. Because the MFO algorithm has the advantages of good globality, IMF²O² adds a perturbation mechanism to avoid the problem of premature convergence in the later stage and improve performance. In addition, the fitness function of the IMF²O² scheme comprehensively considers the network coverage and connectivity rates. If the membership value of the network coverage rate is not greatly improved but the network connectivity value is larger, then the program with better network connectivity rate is preferred, whereas the fitness function of the PSSD scheme only considers the network coverage. The network coverage rate defined in the RAWs scheme is the ratio of the number of nodes covering the monitored event points to the total number of nodes. It determines whether the node covers the target monitoring point, and if it does not cover it, it moves toward the neighbor nodes covering the event point, thus only increasing the number of nodes monitoring the same event point without any increase in the number of unmonitored event points, which does not improve the network coverage rate defined in this

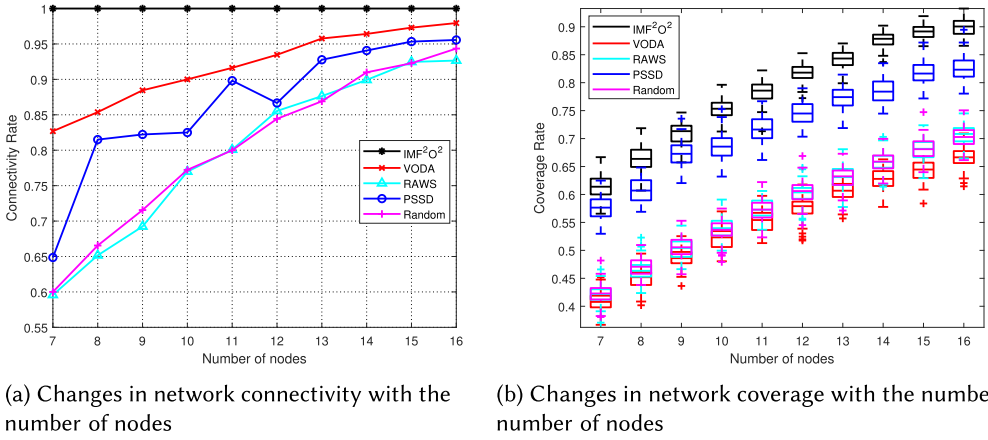


Fig. 8. Network coverage and network connectivity rates under different number of nodes.

article. VODA adjusts the depth of nodes to reduce the coverage overlap area while ensuring relative full connectivity, achieving poor coverage performance. IMF²O² improved network coverage rate by 10%, 22%, and 25% as compared to PSSD, RAWS, and VODA, respectively, while ensuring full connectivity.

Figure 8 shows network coverage and connectivity rates under different number of nodes. We randomly and uniformly distribute 200 target monitoring points for testing. Figure 8(a) depicts the relationship between the number of nodes deployed in different node deployment schemes and the network connectivity rate. The network connectivity rate increases with the number of nodes, but IMF²O² always remains fully connected. When the number of nodes increases to 16, the network connectivity rate of other schemes also reaches about 90%, but the number of nodes is sacrificed for connectivity, which increases the deployment cost. Figure 8(b) portrays the relationship between the number of nodes deployed in different node deployment schemes and the network coverage rate. The network coverage increases with the number of nodes and the growth rate becomes progressively slower, with IMF²O² having the largest network coverage.

6 CONCLUSION

Inspired by the theory of fuzzy mathematics, this article proposes the node deployment method IMF²O² for target monitoring in a 3D underwater environment. The number of nodes is first initialized randomly according to a range of acceptable node deployments by the user, and the problem of obtaining optimal performance with a fixed number of nodes is regarded as an optimization problem. Second, the IMFO algorithm is proposed to implement an optimized node deployment scheme under a fixed number of nodes. In designing the fitness function of the IMFO algorithm, the fuzzy operator is introduced and an objective function based on the fuzzy operator is designed to solve the problem of lack of simultaneous consideration of network coverage and network connectivity in the existing scheme and realize node fully connected deployment. Finally, with full connectivity, the objective functions of the number of nodes and coverage rate are designed using fuzzy operators to assess whether the peak is reached. If the peak is reached, then the optimal number of nodes and its deployment scheme are obtained; otherwise, the number of nodes is updated using the gradient search method until the peak is reached.

This article introduces the concept of fuzzy operators, and the proposed node deployment scheme achieves high coverage performance with as few sensor nodes as possible while ensuring full connectivity. The experimental results show that the proposed method achieves better

performance than existing schemes. The next step is determining how to implement distributed node deployment based on the work of this article, simulating the effect of water flow on nodes in practical applications, and verifying the effect of water flow on the deployment method.

REFERENCES

- [1] Faiza Al-Salti, Khaled Day, Nasser Alzeidi, and Abderezak Touzene. 2018. Multiple sink placement strategy for underwater wireless sensor networks. In *International Symposium on Networks, Computers and Communications (ISNCC'18)*. 1–6.
- [2] Hesham Alhumyani, Reda A. Ammar, Raafat S. Elfouly, and Ayman Alharbi. 2015. Heuristic approaches for underwater sensing and processing deployment. In *11th International Computer Engineering Conference (ICENCO'15)*. 86–91.
- [3] D. Arivudainambi, Sethuraman Balaji, and T. S. Poorani. 2017. Sensor deployment for target coverage in underwater wireless sensor network. In *International Conference on Performance Evaluation and Modeling in Wired and Wireless Networks (PEMWN'17)*. 1–6.
- [4] Fatma Bouabdallah, Chaima Zidi, and Raouf Boutaba. 2017. Joint routing and energy management in UnderWater acoustic sensor networks. *IEEE Trans. Netw. Serv. Manag.* 14 (2017), 456–471.
- [5] Patrick Carroll, Kaleel Mahmood, Shengli Zhou, Hao Zhou, Xiaoka Xu, and Jun-Hong Cui. 2014. On-demand asynchronous localization for underwater sensor networks. *IEEE Trans. Sig. Process.* 62, 13 (2014), 3337–3348.
- [6] Keyu Chen, Maode Ma, En Cheng, Fei Yuan, and Wei Su. 2014. A survey on MAC protocols for underwater wireless sensor networks. *IEEE Commun. Surv. Tutor.* 16 (2014), 1433–1447.
- [7] Huazheng Du, Na Xia, and Rong Zheng. 2014. Particle swarm inspired underwater sensor self-deployment. *Sensors* 14 (2014), 15262–15281.
- [8] Yanzhi Du. 2020. Method for the optimal sensor deployment of WSNs in 3D terrain based on the DPSOVF algorithm. *IEEE Access* 8 (2020), 140806–140821.
- [9] Zabih Ghassemlooy, Shlomi Arnon, Murat Uysal, Zhengyuan Xu, and Julian Cheng. 2015. Emerging optical wireless communications—advances and challenges. *IEEE J. Select. Areas Commun.* 33 (2015), 1738–1749.
- [10] Hari Prabhat Gupta, Pankaj Kumar Tyagi, and Mohinder Pratap Singh. 2015. Regular node deployment for k -coverage in m -connected wireless networks. *IEEE Sensors J.* 15 (2015), 7126–7134.
- [11] Guangjie Han, Jinfang Jiang, Ning Sun, and Lei Shu. 2015. Secure communication for underwater acoustic sensor networks. *IEEE Commun. Mag.* 53 (2015), 54–60.
- [12] Guangjie Han, Chenyu Zhang, Lei Shu, and Joel J. P. C. Rodrigues. 2015. Impacts of deployment strategies on localization performance in underwater acoustic sensor networks. *IEEE Trans. Industr. Electron.* 62 (2015), 1725–1733.
- [13] Guangjie Han, Chenyu Zhang, Lei Shu, Ning Sun, and Qingwu Li. 2013. A survey on deployment algorithms in underwater acoustic sensor networks. *Int. J. Distrib. Sensor Netw.* 9 (2013).
- [14] Shuai Han, Jin Yue, Weixiao Meng, and Xuanli Wu. 2016. A localization based routing protocol for dynamic underwater sensor networks. In *IEEE Global Communications Conference (GLOBECOM'16)*. 1–6.
- [15] Zhanjun Hao, Nanjiang Qu, Xiao chao Dang, and Jiaojiao Hou. 2019. RSS-based coverage deployment method under probability model in 3D-WSN. *IEEE Access* 7 (2019), 183091–183104.
- [16] Ahmed Mohamed Helmi and Ahmed Alenany. 2020. An enhanced moth-flame optimization algorithm for permutation-based problems. *Evolut. Intell.* 13 (2020), 741–764.
- [17] Kaoru Hirota. 1988. Fuzzy theory and its application. *J. Japan Societ. Precis. Eng.* 54 (1988), 2266–2269.
- [18] Junjie Huang, Lijuan Sun, Xun Wei, Peng Sun, Haiping Huang, and Ru chuan Wang. 2014. Redundancy model and boundary effects based coverage-enhancing algorithm for 3D underwater sensor networks. *Int. J. Distrib. Sensor Netw.* 10 (2014).
- [19] Imad Jawhar, Nader Mohamed, Jameela Al-Jaroodi, and Shengyou Zhang. 2019. An architecture for using autonomous underwater vehicles in wireless sensor networks for underwater pipeline monitoring. *IEEE Trans. Industr. Inform.* 15 (2019), 1329–1340.
- [20] Peng Jiang, Yang Feng, and Feng-Nien Wu. 2016. Underwater sensor network redeployment algorithm based on wolf search. *Sensors* 16 (2016).
- [21] Peng Jiang, Jun Liu, Binfeng Ruan, Lurong Jiang, and Feng-Nien Wu. 2016. A new node deployment and location dispatch algorithm for underwater sensor networks. *Sensors* 16 (2016).
- [22] Zhigang Jin, Zhihua Ji, Yishan Su, Shuo Li, and Boyao Wei. 2018. A deployment optimization mechanism using depth adjustable nodes in underwater acoustic sensor networks. In *OCEANS - MTS/IEEE Kobe Techno-Oceans (OTO'18)*. 1–6.
- [23] Chih-Wei Kang and Jian-Hung Chen. 2009. An evolutionary approach for multi-objective 3D differentiated sensor network deployment. In *International Conference on Computational Science and Engineering*. 187–193.

- [24] Zakia Khalfallah, Ilhem Fajjari, Nadjib Aitsaadi, Paul A. Rubin, and Guy Pujolle. 2016. A novel 3D underwater WSN deployment strategy for full-coverage and connectivity in rivers. In *IEEE International Conference on Communications (ICC'16)*. 1–7.
- [25] Sunhyo Kim and Jee Woong Choi. 2017. Optimal deployment of sensor nodes based on performance surface of underwater acoustic communication. *Sensors* 17 (2017).
- [26] Bernhard H. Korte, Jens Vygen, B. Korte, and J. Vygen. 2011. *Combinatorial Optimization*. Vol. 1. Springer.
- [27] Wang Kun, Tian Yuzhen, and Shi Yinhua. 2016. Energy balanced pressure routing protocol for underwater sensor networks. In *International Computer Symposium (ICS'16)*. 216–220.
- [28] Lingfeng Liu, Maode Ma, Chunfeng Liu, and Yantai Shu. 2017. Optimal relay node placement and flow allocation in underwater acoustic sensor networks. *IEEE Trans. Commun.* 65 (2017), 2141–2152.
- [29] Seyed Mohammad Mirjalili. 2015. Moth-flame optimization algorithm: A novel nature-inspired heuristic paradigm. *Knowl. Based Syst.* 89 (2015), 228–249.
- [30] Na Xia, Changsheng Wang, Rong Zheng, and Jianguo Jiang. 2012. Fish swarm inspired underwater sensor deployment. *Acta Automatica Sinica* 38 (2012), 295–302.
- [31] Chun Kit Ng, Chun-Ho Wu, Wai Hung Ip, and Kai-Leung Yung. 2018. A smart bat algorithm for wireless sensor network deployment in 3-D environment. *IEEE Commun. Lett.* 22 (2018), 2120–2123.
- [32] Tajudeen Olawale Olasupo and Carlos E. Otero. 2018. A framework for optimizing the deployment of wireless sensor networks. *IEEE Trans. Netw. Serv. Manag.* 15 (2018), 1105–1118.
- [33] Nasir Saeed, Tareq Y. Al-Naffouri, and Mohamed-Slim Alouini. 2019. Outlier detection and optimal anchor placement for 3-D underwater optical wireless sensor network localization. *IEEE Trans. Commun.* 67 (2019), 611–622.
- [34] Dr. Sandeep and Vinay Kumar. 2017. Review on clustering, coverage and connectivity in underwater wireless sensor networks: A communication techniques perspective. *IEEE Access* 5 (2017), 11176–11199.
- [35] Fatih Senel, Kemal Akkaya, and Turgay Yilmaz. 2013. Autonomous deployment of sensors for maximized coverage and guaranteed connectivity in underwater acoustic sensor networks. In *38th Annual IEEE Conference on Local Computer Networks*. 211–218.
- [36] Jian Shen, Haowen Tan, Jin Wang, Jinwei Wang, and Sungyoung Lee. 2015. A novel routing protocol providing good transmission reliability in underwater sensor networks. *J. Internet Technol.* 16 (2015), 171–178.
- [37] Xiaoli Song, Yun zhan Gong, Dahai Jin, and Qiangyi Li. 2018. Nodes deployment optimization algorithm based on improved evidence theory of underwater wireless sensor networks. *Photon. Netw. Commun.* 37 (2018), 224–232.
- [38] Yishan Su, Lei Guo, Zhigang Jin, and Xiaomei Fu. 2020. A voronoi-based optimized depth adjustment deployment scheme for underwater acoustic sensor networks. *IEEE Sensors J.* 20 (2020), 13849–13860.
- [39] Sai Wang, Thu L. N. Nguyen, and Yoan Shin. 2018. Data collection strategy for magnetic induction based monitoring in underwater sensor networks. *IEEE Access* 6 (2018), 43644–43653.
- [40] Wenming Wang, Haiping Huang, Fan He, Fu Xiao, Xin Jiang, and Chao Sha. 2019. An enhanced virtual force algorithm for diverse k-coverage deployment of 3D underwater wireless sensor networks. *Sensors* 19 (2019).
- [41] Yiyue Wang, Hongmei Li, and Hengyang Hu. 2012. Wireless sensor network deployment using an optimized artificial fish swarm algorithm. In *International Conference on Computer Science and Electronics Engineering*. 90–94.
- [42] Robert Webster, Kumudu S. Munasinghe, and Abbas Jamalipour. 2018. Murmuration inspired clustering protocol for underwater wireless sensor networks. In *IEEE International Conference on Communications (ICC'18)*. 1–6.
- [43] Jing Yan, Xian Yang, Xiaoyuan Luo, and Cailian Chen. 2018. Energy-efficient data collection over AUV-assisted underwater acoustic sensor network. *IEEE Syst. J.* 12 (2018), 3519–3530.
- [44] Hongyu Yang, Yuan Zhou, Yu-Hen Hu, Boyu Wang, and S. Y. Kung. 2018. Cross-layer design for network lifetime maximization in underwater wireless sensor networks. In *IEEE International Conference on Communications (ICC'18)*. 1–6.
- [45] Zhaoquan Zeng, Shu Fu, Huihui Zhang, Yuhan Dong, and Julian Cheng. 2017. A survey of underwater optical wireless communications. *IEEE Commun. Surv. Tutor.* 19 (2017), 204–238.
- [46] Hao Zhang, Shi-Lian Wang, and Haixin Sun. 2016. Research on water surface gateway deployment in underwater acoustic sensor networks. In *OCEANS 2016 MTS/IEEE Monterey*. 1–7.
- [47] Linbo Zhang and M. Motani. 2014. On multicasting in underwater acoustic networks. In *IEEE Global Communications Conference (GLOBECOM'14)*. 1–6.
- [48] Ying Zhang, Mingxing Wang, Jixing Liang, Haiyang Zhang, Wei Chen, and Shengming Jiang. 2017. Coverage enhancing of 3D underwater sensor networks based on improved fruit fly optimization algorithm. *Soft Comput.* 21 (2017), 6019–6029.
- [49] Xia Zun-quan. 2012. n-Dimensional convex fuzzy sets and n-dimensional fuzzy numbers. *J. Dalian Univ. Technol.* (2012).

Received 16 May 2022; revised 14 October 2022; accepted 15 December 2022